AIP | Review of Scientific Instruments

A cryostat for low-temperature spectroscopy of condensable species

E. Carrasco, J. M. Castillo, R. Escribano, V. J. Herrero, M. A. Moreno et al.

Citation: Rev. Sci. Instrum. **73**, 3469 (2002); doi: 10.1063/1.1505658
View online: http://dx.doi.org/10.1063/1.1505658
View Table of Contents: http://rsi.aip.org/resource/1/RSINAK/v73/i10
Published by the AIP Publishing LLC.

Additional information on Rev. Sci. Instrum.

Journal Homepage: http://rsi.aip.org
Journal Information: http://rsi.aip.org/about/about_the_journal
Top downloads: http://rsi.aip.org/features/most_downloaded
Information for Authors: http://rsi.aip.org/authors

ADVERTISEMENT

Downloaded 04 Sep 2013 to 161.111.22.173. This article is copyrighted as indicated in the abstract. Reuse of AIP content is subject to the terms at: http://rsi.aip.org/about/rights_and_permissions

A cryostat for low-temperature spectroscopy of condensable species

E. Carrasco, J. M. Castillo, R. Escribano, V. J. Herrero, M. A. Moreno, and J. Rodríguez
Instituto de Estructura de la Materia (CSIC), Serrano 123, 28006 Madrid, Spain

(Received 18 February 2002; accepted for publication 16 July 2002)

A simple experimental setup for the production of cold samples for spectroscopy is described. The samples are deposited under vacuum on a cold metallic surface whose temperature is controlled between 80 and 323 K by varying the heat flow balance between a liquid nitrogen reservoir and a power transistor. Tests of temperature stability and thermal inertia, as well as a set of reflection–absorption infrared and thermal desorption spectra, are reported as a demonstration of the performance of the system. © *2002 American Institute of Physics.* [DOI: 10.1063/1.1505658]

I. INTRODUCTION

Since its inception in the 1950s,[1] the matrix isolation technique, based on the dilution of the sample of interest in an inert gas which is then frozen to give a rigid solid, has found widespread application in spectroscopic laboratories, specially for the study of trace gases and of unstable or chemically reactive species (see, for instance, Ref. 2 and references therein). Rare gases and molecular nitrogen offer great advantages for the formation of matrices due to their transparency over an extended spectral range and to their chemical inertness; however, temperatures below 20 K are needed in order to attain the adequate rigidity and to prevent diffusion. Sophisticated compression or liquid He cryostats are then required.

Later developments of the matrix isolation technique have shown the possibility of using ''unconventional'' substances like H_2O or CO_2 in association with specific detection techniques (electron spin resonance[3,4] in the case of water, and infrared (IR) spectroscopy[2,5] in the case of CO_2). The formation of water and CO_2 matrices requires just the use of liquid nitrogen (77 K) instead of liquid He, which offers many practical and cost-reducing advantages. Solid CO_2 can be particularly convenient for spectroscopic studies of trace gases with IR spectroscopy. At liquid nitrogen temperature, CO_2 matrices are sufficiently stable and rigid and do not allow a significant diffusion of the trace gas molecules diluted in them. In the 800–3600 cm^{-1} interval, broad strong absorptions take place only between 2200 and 2400 cm^{-1}. Over the rest of this spectral range the CO_2 matrix is transparent with just a few narrow absorption features or weakly absorbing broadbands corresponding to lattice vibrations that do not interfere with the absorption lines of many trace gases. In addition, some of the narrow absorptions of CO_2 can be used as an internal calibration for the quantitative determination of unknown trace gas concentrations.[2]

In recent times, the study of the structure and properties of ''ices'' of different condensable species has attracted much attention, specially in connection with the investigation of heterogeneous processes in the upper atmosphere.[6,7] In particular, solid films of water and of hydrates of nitric acid, and sometimes also of sulphuric acid, intended to mimic the composition of the particles present in polar stratospheric clouds, have been investigated by various groups at the atmospheric relevant temperatures ($T < 180–200$ K). Several experimental techniques including Fourier transform infrared (FTIR) spectroscopy, temperature programmed desorption (TPD), and transmission electron microscopy are being used for the investigation of the structure, changes in morphology, thermodynamics and kinetics of formation, and evaporation of these solid layers (see for instance Refs. 8–15 and the references cited therein).

The kind of studies commented on in the previous paragraphs requires a cryostatic setup for the preparation of the samples of interest. In the present work we describe the construction of a low cost uncomplicated system for the deposition and temperature control of cold samples. The system can operate between 80 and 323 K and is controlled with a computer program. Tests of the temperature stability and thermal inertia are presented in this article. As a check of its performance we present measurements of trace amounts of N_2O diluted in a CO_2 matrix and also reflection–absorption infrared (RAIR) and thermal desorption spectra of solid water films.

II. INSTRUMENTAL SETUP

A. High vacuum chamber and cryostat

A general scheme of the instrument is shown in Fig. 1. The samples of interest are deposited on the polished surface (mirror) of a 3 mm thick aluminum plate (substrate), which is fixed with two screws to a mount in contact with a copper block. The same mount contains the heating element, a power transistor of a popular type (2N3055) capable of providing enough power for the present needs (which never exceed 60 W), and whose upper cover is in contact with the back face of the Al plate. The tightening of the screws fixing the Al substrate to the mount, causes it to be pressed against the flat transistor cover. The use of this power transistor offers an interesting alternative to the conventional resistive heating. It allows a very good and uniform thermal contact, since the heat is released directly to the aluminum plate from the transistor cover whose surface nearly matches in size that of the substrate. The copper block holding the mount with the substrate is screwed to the bottom of a liquid nitrogen vessel welded to the 150 conflat (CF) flange that closes the

 © 2002 American Institute of Physics

Downloaded 04 Sep 2013 to 161.111.22.173. This article is copyrighted as indicated in the abstract. Reuse of AIP content is subject to the terms at: http://rsi.aip.org/about/rights_and_permissions

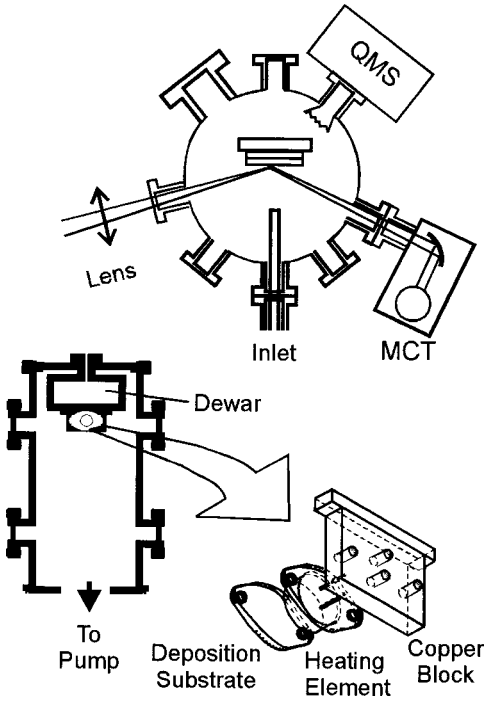

FIG. 1. Scheme of the vacuum chamber and cryostat. The inset shows the assembly of the heating element (power transistor) and the metallic substrate for the deposition of the samples; QMS: quadrupole mass spectrometer, MCT: mercury–cadmium–telluride IR detector.

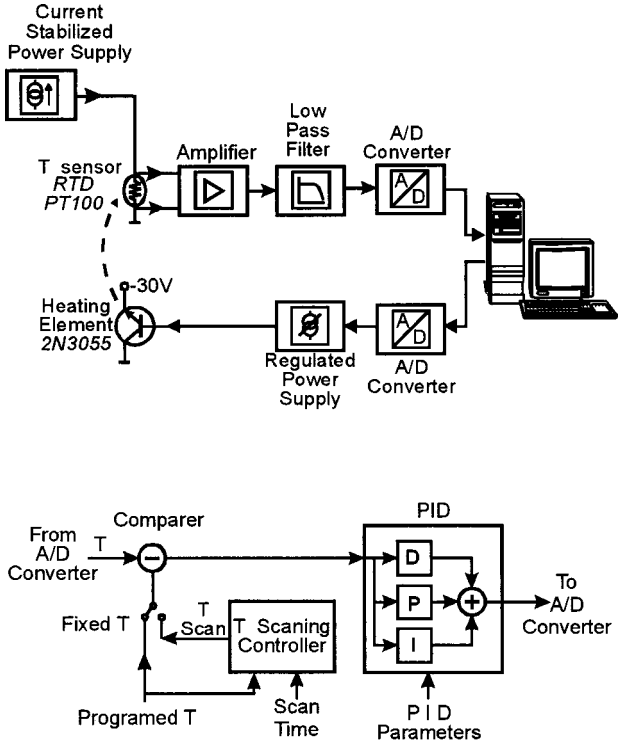

FIG. 2. Block diagram of the automated temperature control system.

upper end of the chamber. The contact at the various metallic surfaces is improved by placing between them narrow tin foils before tightening the supporting screws. The temperature is monitored at two places, the Al substrate (T_1) and the copper block (T_2), by means of two Pt-100 resistances, housed in holes specially built to match the size of the sensors. The substitution of the substrate or the conducting copper block by other materials with different thermal or chemical properties is straightforward.

The cylindrical chamber wall has eight openings provided with CF ultrahigh vacuum flanges. Seven of these flanges correspond the 35 CF standard and are meant for the installation of IR windows, electrical feedthroughs, entrances for the gases or vapors to be deposited, and for the installation of a small quadrupole mass spectrometer (QMS). The eighth flange is larger (100 CF) and is intended for the final adjustment of the optical alignment of the mirror and of the electrical connections. The relative orientation of the various openings is such that both transmission and reflection–absorption spectroscopy, with a reflection angle of 75°, are possible. The chamber is evacuated by means of a turbomolecular pump (Pfeiffer/Balzers TMU261) with a nominal pumping speed of 210 $\mathrm{l\,s^{-1}}$ for N_2. This pump is backed by a 5.5 $\mathrm{m^3\,h^{-1}}$ rotary pump. The typical background pressure in the chamber (without baking and without liquid nitrogen in the reservoir) is $<3\times10^{-8}$ mbar. After filling the liquid nitrogen vessel, the background pressure is in the 10^{-9} mbar range.

Different possibilities can be used for the deposition of the samples of interest. For some of the experiments described below we have connected, at the inner side of the gas inlet flange, a stainless steel tube ending in a 0.5 mm hole placed at a short distance (2–3 cm) of the metallic mirror and oriented directly toward its surface. In other experiments a curved tube was used in order to deviate the direct gas flow toward the chamber walls and produce a slower, more homogeneous deposition by filling the whole chamber with a vapor of the condensable species. Other deposition possibilities like the use of pulsed valves or effusive molecular beams can be easily implemented, but have not been tried in the test experiments reported in the next section.

B. Temperature control

The temperature is controlled with a computer program. A scheme of the electronic control circuitry is shown in Fig. 2. The signals provided by the Pt-100 temperature sensors are led through signal conditioners that deliver a voltage proportional to the temperature (i.e. the sensor resistance) to an analog to digital (A/D) converter connected directly to the computer. The actual temperatures of the metallic substrate T_1 and of the copper block T_2 are displayed on the computer screen, and on this same screen the desired temperature of the metallic substrate is selected. The driving program calculates the difference between the actual and the desired substrate temperatures ΔT_1 and acts upon a software implemented proportional integral differential controller with a direct output to a D/A converter. The ΔT_1 signal generated controls the current through the heating element. The arrangement of the power transistor (heating element) is not the usual one, but it was adopted because the transistor used is of the negative positive negative (NPN) type with its collector in contact with the case which, in the present setup, must be grounded in order to meet the thermal conduction requirements. For this reason, a special excitation circuit was

Downloaded 04 Sep 2013 to 161.111.22.173. This article is copyrighted as indicated in the abstract. Reuse of AIP content is subject to the terms at: http://rsi.aip.org/about/rights_and_permissions

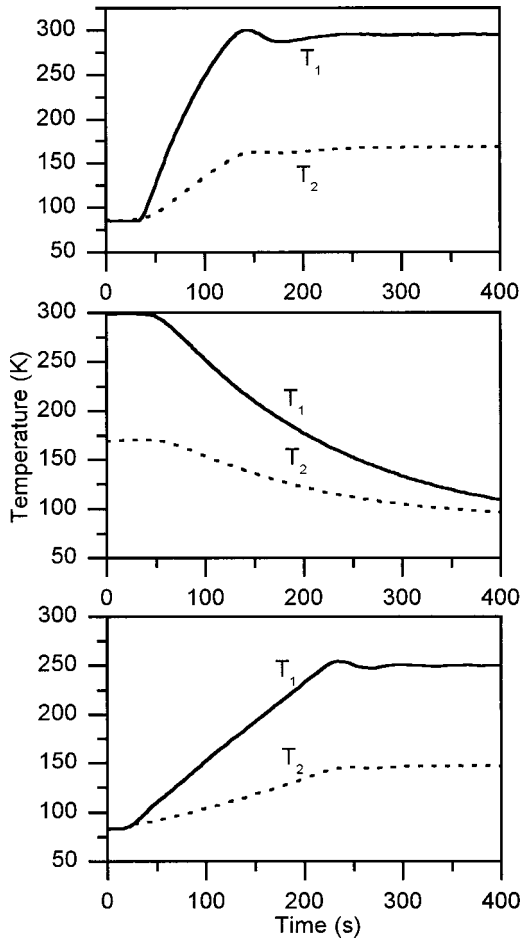

FIG. 3. Time evolution of the temperatures of the metallic deposition substrate (T_1) and of the copper block (T_2) between the substrate and the liquid nitrogen reservoir: (Upper panel) direct (fastest) heating; (Middle panel) direct cooling; and (Lower panel) heating of the deposition substrate at a rate of 50 K/min.

designed in order to control the current through the transistor with the emitter connected to -30 V. In any case, the collector–emitter current is regulated by controlling the base current I_b as a function of the ΔT_1 signal generated by the A/D converter. Under the experimental conditions of interest the needed I_b is obtained with a base–emitter voltage ranging from approximately 0.8 V at $T_1 = 290$ K to 1.2 V at $T_1 = 95$ K.

Figure 3 shows curves for the time evolution of the relevant temperatures (T_1, T_2) for the interval 85–300 K during various heating and cooling processes. The upper panel shows the curves for ''direct'' heating (i.e., with the heating element always on until the desired temperature is reached). In the present case a final temperature of 296 K was selected in the program. The small mass of the substrate results in a small thermal inertia, which allows a quick temperature variation. Once the programmed temperature is reached, it gets stabilized to better than 1 K in a few minutes ($\approx$3 min in the extreme case depicted in the upper panel). After the stabilization at the final temperature, the heating element was disconnected. The resulting process of ''direct'' cooling is represented in the middle panel. As can be seen by comparing these two graphs, the heating is faster due to the fact that the heat is directly liberated in the close vicinity of the metallic substrate, whereas the cooling takes longer since the excess heat must flow in a slower way toward the liquid nitrogen reservoir. In any case, only 10 min are needed to cool the substrate from room temperature to 90 K.

A linear temperature variation is often convenient for operation. This is the case for instance in the studies of TPD. In this type of experiment the rate of evaporation is recorded as a function of the sample temperature and a linear heating rate simplifies the analysis of the data. The temperature increase must be relatively fast in order to produce an evaporation of the sample of interest without inducing structural changes in it. In the lowest panel of Fig. 3, a linear temperature increase of 50 K/min has been selected, which is a typical value in TPD experiments. In order to achieve the appropriate temperature variation, the software takes the desired rate of temperature increase and divides the total temperature increment ΔT into a series of smaller intermediate steps giving a linear evolution of T with time. For the tests reported in this article a time step of 1 s was used. The example shown in this figure corresponds to the rate of temperature variation employed in the thermal desorption spectroscopy measurements described in Sec. III. It is worth noting that the difference between T_1 and T_2 is large enough as to ensure that the programmed desorption will take place just at the deposition substrate and not on the copper block. If necessary, this temperature difference can be made larger by substituting the copper block by other material with a smaller thermal conductivity.

III. EXPERIMENTAL TESTS

In order to demonstrate the performance of the present cryostatic system we report in this section some experiments with representative cold samples deposited on the substrate. The two upper panels of Fig. 4 show RAIR spectra of N_2O traces in a CO_2 matrix and of water ice layers of different thickness, respectively. The lowest panel displays the TPD of water (ice) from the Al substrate. The RAIR spectra have been recorded with a FTIR spectrometer Brucker IFS66. The radiation of the Globar source is deflected with a mirror from the standard sample compartment of the spectrometer and focused with a CaF_2 lens on the sample inside the chamber. The use of this lens sets a lower limit of approximately 1000 cm^{-1} to the available spectral range. The IR beam enters and leaves the chamber through two KBr windows and has an angle of incidence of 75° with respect to the deposition surface. After leaving the chamber, the reflected IR radiation is focused by means of a mirror onto a mercury–cadmium–telluride (MCT) detector refrigerated with liquid nitrogen. The TPD of water was monitored by following the evolution of the $m/q = 18$ peak as recorded with a QMS (Leybold Transpectror C-100) installed in one of the ports of the deposition chamber. As indicated above, a heating rate of 50 K/min was selected for these experiments.

A mixture of N_2O and CO_2 with an approximate mixing ratio $\mu_{N_2O} = (1 \pm 0.1) \times 10^{-3}$ was prepared in a sample cylinder. This proportion is roughly that of the atmosphere where N_2O and CO_2 have typical concentrations of 300 ppb

Downloaded 04 Sep 2013 to 161.111.22.173. This article is copyrighted as indicated in the abstract. Reuse of AIP content is subject to the terms at: http://rsi.aip.org/about/rights_and_permissions

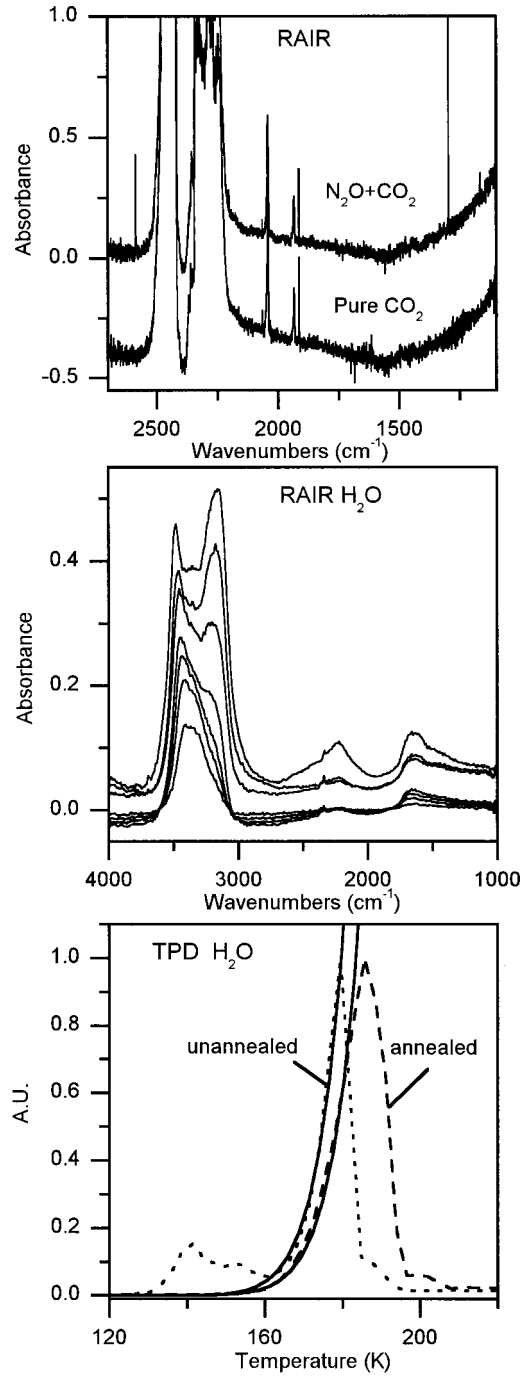

FIG. 4. Experimental tests: (Top panel) RAIR spectra of CO_2 matrices deposited at 85 K. The upper spectrum corresponds to a mixture of about 0.1% N_2O in CO_2. The lower spectrum is a reference spectrum of pure CO_2. The absorbances represented correspond to base *e* logarithms. The absorbance scale has been cut at one and the spectrum of pure CO_2 has been shifted for convenience of display. (Middle panel) RAIR spectra of water layers of different thickness deposited at 85 K. (Bottom panel) TPD spectra of an annealed (dashed line) and an unannealed (dotted line) thin water film. The mass spectrometer output signals have been normalized to one at the maximum. The heating rate corresponding to this spectra is shown in the lower panel of Fig. 3. The solid lines are a fit of a zero order desorption rate to the data.

and 350 ppm, respectively. The sample was then let in the cylinder for 48 h before recording the spectra; after this time the mixture is expected to be homogeneous. The mixture thus prepared was expanded into the vacuum chamber and condensed on the cold (80 K) substrate. Under these conditions the individual N_2O molecules should be separated by approximately 10 matrix molecules in each direction and thus sufficiently isolated from each other. The velocity of deposition is essentially determined by the gas pressure in the chamber P_c, which is in turn given by the equilibrium between the gas flow (regulated with a valve at the entrance) and the pumping speed of the vacuum pump. For the spectra commented on in the next paragraph, typical P_c values of 5×10^{-2} mbar (direct pirani gauge measurement) and a deposition time of 10 s were used. These conditions lead a CO_2 layer with an effective absorbing length of 40–50 μm (see below).

The RAIR spectrum of the N_2O/CO_2 matrix in the 1100–2700 cm^{-1} range is displayed in the upper panel of Fig. 4 together with that of a reference matrix of pure CO_2. In these spectra, there is a region of strong absorption, corresponding to the ν_3 band of solid CO_2, between 2200 and 2500 cm^{-1}. Some weak CO_2 absorptions can be also identified in the region between 1800 and 2100 cm^{-1}. Over the rest of the spectral range shown, the CO_2 matrix is essentially transparent. The weak CO_2 features can be used to estimate the approximate absorbing thickness d of the matrix by using the simple relationship: $A_{CO_2}=\alpha_{CO_2}d$, where A_{CO_2} is the integrated absorbance of a given line and α_{CO_2} its absorption coefficient. Taking the α values listed in Ref. 2 for the absorption lines at 1834 and 1814 cm^{-1} (5.87×10^{-3} and 2.36×10^{-2} $cm^{-1}\,\mu m^{-1}$, respectively), one gets an effective absorption thickness of about 40–50 μm for the CO_2 matrix. In the upper spectrum, the ν_1 band of N_2O in the matrix appears as an intense absorption at 1297 cm^{-1}. This frequency is shifted by 12 cm^{-1} with respect to the corresponding gas phase value and coincides with the matrix shift reported in Ref. 2. The N_2O spectrum also contains a weaker peak at 2586 cm^{-1} ($2\nu_1$), which can be used to monitor the N_2O content in a sample. In our case, where the N_2O concentration is known, a comparison of the A_{N_2O} integrated absorbance at this frequency with the A_{CO_2} absorptions mentioned above can lead to the determination of the α_{N_2O} (2586 cm^{-1}) coefficient in the matrix. Conversely, the use of a tabulated value of this coefficient ($\alpha_{N_2O}=6.6\pm0.12\,cm^{-1}\,\mu m^{-1}$, from Ref. 2) and the absorption ratio between the N_2O and CO_2 bands, leads to the evaluation of the N_2O concentration. In our spectra, the value thus obtained would be $(1.3\pm0.3)\times10^{-3}$ for the mixing ratio of N_2O in the matrix, in reasonable agreement with the concentration initially prepared.

RAIR spectra of amorphous water ice collected at 85 K are shown in the middle panel of Fig. 4 for ice films of increasing thickness deposited on the Al substrate. These spectra are in good agreement with previous RAIR spectra recorded under large incidence angle.[11,12,16,17] The thickness of the ice films can be estimated by different methods,[12] and for the present experiments should range from about 50 nm to some μm. However, the estimates of the film width have led to controversial results especially for the thickest layers.[12,16] In the range covered by the present measurements the spectra consist of a strong broadband in the 3000–3500

Downloaded 04 Sep 2013 to 161.111.22.173. This article is copyrighted as indicated in the abstract. Reuse of AIP content is subject to the terms at: http://rsi.aip.org/about/rights_and_permissions

cm^{-1} region, corresponding to the coupled OH stretching modes (ν_1, ν_3) and of two weak bands, one of them with a maximum at about 2240 cm^{-1} attributed to the third overtone of the librational mode ($3\nu_L$), and the other one with a maximum at approximately 1650 cm^{-1} due to the bending mode (ν_2) of H_2O with a possible contribution of the second librational overtone ($2\nu_L$).[11]

For the thinnest films, a single band, peaking at ≈3415 cm^{-1}, is observed in the OH stretching region. With growing thickness, the band becomes wider and eventually develops a second peak at ≈3170 cm^{-1}, which becomes dominant for the thickest layers. The appearance of these two features has been interpreted in terms of the interaction of the IR radiation with longitudinal optical (LO) and transverse optical (TO) surface modes in the film.[12,16,17] For the very thin films, the TO mode, giving rise to a transition dipole moment parallel to the surface, is suppressed due to the metal surface selection rule,[16] and only the LO mode, with a transition dipole mode normal to the surface is observed. As the thickness of the film is increased, the metal surface selection rule ceases to apply, the TO mode begins to be excited by the IR radiation, and a second peak appears at lower frequencies in the spectrum. The TO mode is the only one that can be excited in transmission[18] or in low incidence angle RAIR,[14] where it appears as a broadband with a maximum at 3240–3250 cm^{-1}. This frequency is somewhat higher than that of the feature attributed to the absorption of the TO mode in the large-angle incidence RAIR spectra. The reason for this difference is not clear,[14] but it might be related to the persistence of the LO modes for large-angle incidence or to the appearance of optical distortions in the spectra of the thickest films.[17] In spite of the continuing work by different groups, there are still open questions concerning the interpretation of the IR spectra of ice in the OH stretching region.[14,19]

The deposition of water vapor on the 85 K cold substrate produces an amorphous solid I_a. When the temperature of the substrate is increased, this solid undergoes various structural modifications. At $T=120-140$ K a glass transition takes place, by which the amorphous solid transforms into a viscous liquid.[11,20] At $T\approx150$ K a cubic polycrystalline solid I_c begins to form, although much of the deposited film remains as viscous liquid or amorphous solid until temperatures as high as 210 K. This partial crystallization leads to a more stable form of water with a higher surface binding energy. Temperature programmed desorption can be used to monitor these changes in the structure of the deposited ice with temperature.

In the lower panel of Fig. 4 the QMS signal as a function of temperature is displayed for two different samples. The first sample is a thin film of amorphous ice deposited at 85 K. The direct desorption of this sample, shown as a dotted line, gives a small structure peaking at about 140 K, the region of the glass transition of water; after this maximum the signal declines gently until 160 K; beyond this temperature, the evaporation rate rises abruptly reaching a maximum at about 179 K and then falls sharply to zero, after all water has evaporated. The second sample corresponds to a thin water film initially deposited at 85 K, then annealed at 155 K during 20 min, and finally cooled again at 85 K. The annealing procedure induces crystallization and changes irreversibly the structure of the film; in this case a single desorption peak (dashed line), centered at about 186 K is observed. The location of the present desorption maxima is similar to that found in the literature for TPD experiments performed under similar conditions.[11,17] The fact that the desorption of the annealed film takes place at a higher temperature than that of the unannealed sample is a reflection of the higher barrier to evaporation associated with the I_c form of ice.

The desorption of multilayer films of a pure substance from a surface should obey approximately zero order kinetics. This zero order desorption rate can be described by an Arrhenius equation of the form: $v_d = A\exp(-E_d/RT)$, where A is a constant, E_d is the activation energy for desorption, and R is the gas constant. By fitting the rising portion of the TPD curves to this Arrhenius law, E_d values of 9.4 ± 0.4 and 9.8 ± 0.2 kcal/mol are obtained for the unannealed and annealed films, respectively. The fits are shown as solid lines in the bottom panel of Fig. 4. These values are consistent with those of Ref. 21, but are lower by 15%–20% than most of the literature values for crystalline ice (see Ref. 15 and references therein). The E_d increase obtained upon annealing of the freshly deposited ice film is similar to that reported previously by other groups.[20,21]

ACKNOWLEDGMENTS

This work was financed by the MCT of Spain under Grant No. REN 2000-1557 CLI. The authors are indebted to Professor Sodeau for providing them with a copy of Ref. 17, and to Dr. C. Domingo for help with the FTIR spectrometer.

[1] E. Whittle, D. A. Dows, and G. C. Pimentel, J. Chem. Phys. **22**, 1843 (1954).
[2] D. W. T. Griffith, in *Air Monitoring by Spectroscopic Techniques*, edited by M. W. Sigrist (Wiley, New York, 1994). Chap. 7.
[3] M. Helten, W. Pätz, M. Trainer, H. Farke, E. Klein, and D. H. Ehhalt, J. Atmos. Chem. **2**, 181 (1984).
[4] D. Mihelcic, P. Müsgen, and D. H. Ehhalt, J. Atmos. Chem. **3**, 341 (1985).
[5] D. W. T. Griffith and G. Schuster, J. Atmos. Chem. **5**, 59 (1987).
[6] J. R. Sodeau, in *Spectroscopy in Environmental Science*, edited by R. J. H. Clark and R. E. Hester (Wiley, New York, 1995), p. 349.
[7] M. A. Zondlo, P. K. Hudson, A. J. Prenni, and M. A. Tolbert, Annu. Rev. Phys. Chem. **51**, 473 (2000).
[8] G. Ritzhaupt and J. P. Devlin, J. Phys. Chem. **95**, 90 (1991).
[9] G. Koehler, A. Middlebrook, and M. A. Tolbert, J. Geophys. Res. **97**, 8065 (1992).
[10] S. Peil, S. Seisel, and O. Schrems, J. Mol. Struct. **348**, 449 (1995).
[11] P. Jenniskens, S. F. Banham, D. F. Blake, and M. R. S. McCoustra, J. Chem. Phys. **107**, 1232 (1997).
[12] M. A. Zondlo, T. B. Onasch, M. S. Warshawsky, and M. A. Tolbert, J. Phys. Chem. B **101**, 10887 (1997).
[13] R. T. Tisdale, A. M. Middlebrook, A. J. Prenni, and M. A. Tolbert, J. Phys. Chem. A **101**, 2112 (1997).
[14] L. Schriver-Mazzuoli, A. Schriver, and A. Hallou, J. Mol. Struct. **554**, 289 (2000).
[15] B. K. Koehler, Int. J. Chem. Kinet. **33**, 295 (2001).
[16] A. B. Horn, S. F. Banham, and M. R. S. McCoustra, J. Chem. Soc., Faraday Trans. **91**, 4005 (1995).
[17] S. Banham, Ph.D. thesis, University of East Anglia, 1995.
[18] M. S. Bergen, D. Schuh, M. G. Seats, and S. Rice, J. Chem. Phys. **69**, 3477 (1978).
[19] V. Buch and J. P. Devlin, J. Chem. Phys. **110**, 3437 (1999).
[20] R. J. Speedy, P. G. Debenedetti, R. Smith, C. Huang, and B. D. Kay, J. Chem. Phys. **105**, 240 (1996).
[21] S. A. Sandford and L. J. Allamandola, Icarus **76**, 201 (1988).

Downloaded 04 Sep 2013 to 161.111.22.173. This article is copyrighted as indicated in the abstract. Reuse of AIP content is subject to the terms at: http://rsi.aip.org/about/rights_and_permissions